DIFFRACTION AS A FUNDAMENTAL INGREDIENT IN SOFT SCATTERING

Uri Maor

Collaboration with E. Gotsman and E. Levin

Raymond and Beverly Sackler Faculty of Exact Science

Tel Aviv University, Tel Aviv, 69978, Israel

WORKSHOP ON HIGH ENERGY PHYSICS AT THE LHC:

NEW TRENDS IN HEP

NOVEMBER 3-6, 2014. NATAL/RN-BRAZIL

HISTORIC INTRODUCTION

s channel Unitarity screening considerations date back to the ISR epoch, where they provided a simple way out of seemingly paradoxical traps.

1) Given that non screened σ_{tot} grows with energy, σ_{el} grows faster (optical theorem). With no screening, σ_{el} will, eventually, be larger than σ_{tot}.

2) Elastic amplitude is central in impact parameter b, peaking at b=0. Diffractive amplitudes are peripheral, peaking at large b, geting larger with s.

3) Elastic and diffractive scatterings are dynamically similar. However, the b peripherality of the diffractive channels results in an energy dependence of the diffractive cross sections which is less moderate than the elastic.

40 years latter, estimates of soft scattering require a unified analysis of elastic and diffractive scatterings, incorporating s and t unitarity screenings.

S-CHANNEL UNITARITY

The simplest s-channel unitarity bound on $a_{el}(s,b)$ is obtained from a diagonal re-scattering matrix, where repeated elastic scatterings secure s-channel unitarity, $2Ima_{el}(s,b) = |a_{el}(s,b)|^2 + G^{in}(s,b)$.

i.e. At a given (s,b), $\sigma_{tot} = \sigma_{el} + \sigma_{inel}$. Its general solution is:

$$a_{el}(s,b) = i\left(1 - e^{-\Omega(s,b)/2}\right), \quad G^{in}(s,b) = 1 - e^{-\Omega(s,b)}. \quad \Omega \textbf{ is model dependent.}$$

The output s-unitarity bound is $|\, a_{el}(s,b)\,| \leq 2$, leading to very large total and elastic LHC cross sections, which are not supported by LHC recent data.

In a Glauber/Gribov eikonal approximation, the input opacity $\Omega(s,b)$ is real. It equals to the imaginary part of the input model Born term, a Pomeron exchange in our context. The output $a_{el}(s,b)$ is imaginary.

The consequent bound is $|\, a_{el}(s,b)\,| \leq 1$, which is the black disc bound.

In a single channel eikonal model, the screened cross sections are:

$$\sigma_{tot} = 2\int d^2b\left(1 - e^{-\Omega(s,b)/2}\right), \qquad \sigma_{el} = \int d^2b\left(1 - e^{-\Omega(s,b)/2}\right)^2, \qquad \sigma_{inel} = \int d^2b\left(1 - e^{-\Omega(s,b)}\right).$$

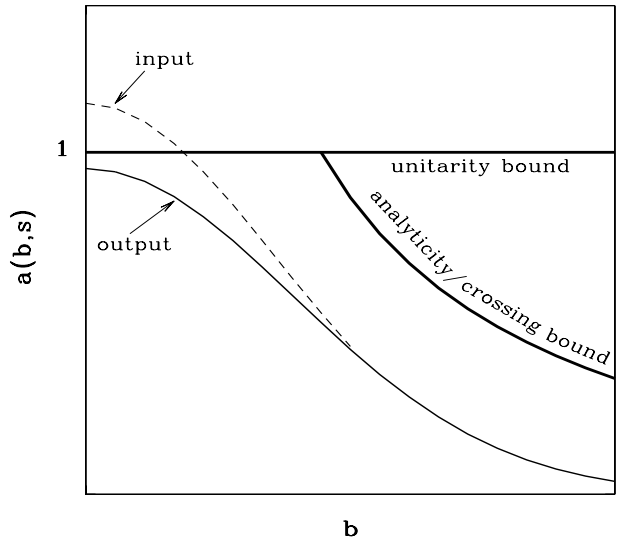

The figure shows the s-channel black bound, and the analyticity/crossing bound implied by the $ln^2(s)$ expanding amplitude radius. The consequent Froissart-Martin bound is: $\sigma_{tot} \leq Cln^2(s/s_0),\ s_0 = 1GeV^2,\ C \propto 1/2m_\pi^2 \simeq 30mb.$

C is far too large to be relevant even at the TeV-scale.

s-unitarity implies: $\sigma_{el} \leq \frac{1}{2}\sigma_{tot}$ and $\sigma_{inel} \geq \frac{1}{2}\sigma_{tot}$. At saturation, $\sigma_{el} = \sigma_{inel} = \frac{1}{2}\sigma_{tot}$.

Introducing diffraction, significantly changes the features of s-unitarity.

However, the saturation signatures, stated above, remain valid.

GOOD-WALKER DECOMPOSITION

Consider a system of two orthonormal states, a hadron Ψ_h and a diffractive state Ψ_D. Ψ_D replaces the continuous diffractive Fock states. Good-Walker (GW) noted that Ψ_h and Ψ_D do not diagonalize the 2x2 interaction matrix T. Let Ψ_1 and Ψ_2 be eigen states of T :

$$\Psi_h = \alpha\Psi_1 + \beta\Psi_2, \quad \Psi_D = -\beta\Psi_1 + \alpha\Psi_2, \quad \alpha^2 + \beta^2 = 1.$$

The eigen states initiate 4 $A_{i,k}$ elastic GW amplitudes $(\psi_i + \psi_k \to \psi_i + \psi_k)$. i,k=1,2. For initial $p(\bar{p}) - p$ we have $A_{1,2} = A_{2,1}$. I shall follow the GLM definition, in which the mass distribution of Ψ_D is not defined and requires a specification.

The elastic, SD and DD amplitudes in a 2 channel screened GW model are:

$$a_{el}(s,b) = i\{\alpha^4 A_{1,1} + 2\alpha^2\beta^2 A_{1,2} + \beta^4 A_{2,2}\},$$

$$a_{sd}(s,b) = i\alpha\beta\{-\alpha^2 A_{1,1} + (\alpha^2 - \beta^2)A_{1,2} + \beta^2 A_{2,2}\},$$

$$a_{dd}(s,b) = i\alpha^2\beta^2\{A_{1,1} - 2A_{1,2} + A_{2,2}\},$$

$$A_{i,k}(s,b) = \left(1 - e^{\frac{1}{2}\Omega_{i,k}(s,b)}\right) \leq 1.$$

Introducing t-channel screening results in a distinction between GW and non GW diffraction. In the GW sector,

- **We obtain the Pumplin bound:** $\sigma_{el} + \sigma_{diff}^{GW} \leq \frac{1}{2}\sigma_{tot}$**.**
  σ_{diff}^{GW} **is the sum of the GW soft diffractive cross sections.**
- **Below saturation,** $\sigma_{el} < \frac{1}{2}\sigma_{tot} - \sigma_{diff}^{GW}$ **and** $\sigma_{inel} > \frac{1}{2}\sigma_{tot} + \sigma_{diff}^{GW}$.
- $a_{el}(s,b) = 1$, **when and only when,** $A_{1,1}(s,b) = A_{1,2}(s,b) = A_{2,2}(s,b) = 1$**.**
- **When** $a_{el}(s,b) = 1$, **all diffractive amplitudes at the same (s,b) vanish.**
- **The saturation signature,** $\sigma_{el} = \sigma_{inel} = \frac{1}{2}\sigma_{tot}$, **in a multi channel calculation is coupled to** $\sigma_{diff} = 0$**. Consequently, prior to saturation the diffractive cross sections stop growing and start to decrease with energy.**
- **The above holds only in a multi channel analysis.**
  It does not hold in a single channel model.
- **GW saturation signatures are valid also in the non GW sector.**

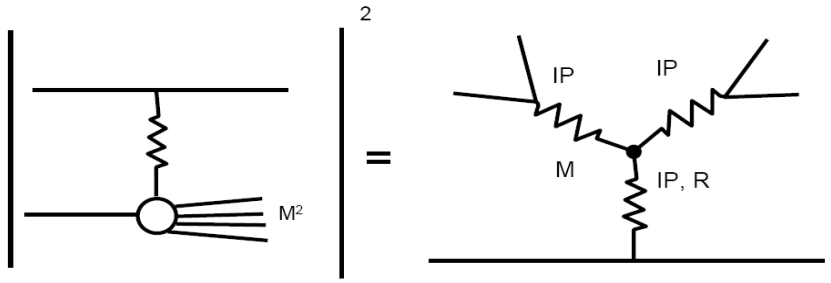

CROSSED CHANNELED UNITARITY

Translating the concepts presented into a viable phenomenology requires a specification of $\Omega(s,b)$, for which Regge Pomeron ($I\!P$) theory is a powerful tool.

Mueller(1971) applied 3 body unitarity to equate the cross section of $a+b \to M_{sd}^2 + b$ to the triple Regge diagram $a+b+\bar{b} \to a+b+\bar{b}$, with a leading $3I\!P$ vertex term.

The $3I\!P$ approximation is valid when $\frac{m_p^2}{M_{sd}^2} << 1$ and $\frac{M_{sd}^2}{s} << 1$.

The leading energy/mass dependences are $\frac{d\sigma^{3I\!P}}{dt\, dM_{sd}^2} \propto s^{2\Delta_{I\!P}} (\frac{1}{M_{sd}^2})^{1+\Delta_{I\!P}}$.

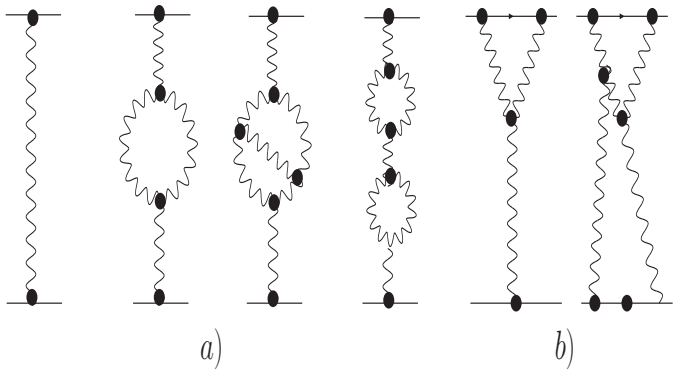

Mueller's 3$I\!P$ approximation for non GW diffraction is the lowest order of t-channel multi $I\!P$ interactions, compatible with t-channel unitarity. Recall that unitarity screening of GW ("low mass") diffraction is carried out explicitly by eikonalization, while the screening of non GW ("high mass") diffraction is carried out by the survival probability (to be discussed).

The figure shows the $I\!P$ Green function. Multi $I\!P$ interactions induce large mass diffraction. Note the analogy with QED.

a) Enhanced diagrams induce the propagator renormalization.

b) Semi enhanced diagrams, present the p$I\!P$p vertex renormalization.

SURVIVAL PROBABILITY

The experimental signature of a $I\!P$ exchanged reaction is a large rapidity gap (LRG), devoid of hadrons in the $\eta - \phi$ lego plot, $\eta = -ln(tan\frac{\theta}{2})$.

S^2, the LRG survival probability, is a unitarity induced suppression factor of non GW diffraction, soft or hard: $S^2 = \sigma_{diff}^{screened}/\sigma_{diff}^{nonscreened}$.

It is the probability that the LRG signature will not be filled with debris (partons and/or hadrons), originating from either the s-channel re-scatterings of the spectator partons, or by the t-channel multi $I\!P$ interactions.

Denote the gap survival factor initiated by s-channel eikonalization S^2_{eik}, and the one initiated by t-channel multi $I\!P$ interactions, $S^2_{mI\!P}$.

The incoming projectiles are summed over (i,k).

S^2 is obtained from a convolution of S^2_{eik} and $S^2_{mI\!P}$.

A simpler, reasonable approximation, is $S^2 = S^2_{eik} \cdot S^2_{mI\!P}$.

INCORPORATING GOOD-WALKER AND MUELLER DIFFRACTIONS

Both the experimental and theoretical studies of soft diffraction are hindered by conflicting definitions of signatures and bounds.

In our context, I wish to discuss the relationship between GW and non GW diffraction versus Mueller's low and high diffractive mass.

Kaidalov, at the time, equated (without a proof) Mueller's low diffractive mass with GW diffraction, and high diffractive mass with non GW diffraction.

The problem is how do we define the bounds of these diffractive mass domains.

Following Kaidalov, GW low mass upper bound and Mueller's high mass lower bound, which is 4-5 GeV, coincide.

i.e. there is no overlap of low and high mass diffraction.

This point of view is shared by KMR, Ostapchenko and Poghosyan.

I find this assumption problematic, as it offers no procedure which secures a smooth behaviour of the diffractive mass through this transition.

In the GLM model the GW diffractive mass is not defined. We presume (also without a proof) that GW and non GW (high mass) diffraction have the same upper bound, commonly taken to be 0.05s.

As we saw, The main difference between the 2 diffractive modes is that GW is suppressed by eikonal screenings, while non GW is suppressed by the survival prrobability which has an s-chanel eikonal component initiated by the re-scattering of the initial projectiles and a t-channel screening induced by the multi $I\!P$ interactions.

In GLM most of the diffraction is GW, while in KMR it is non GW high mass.

Originally, GLM did not define a diffractive mass distribution. This has been amended in one of GLM recent papers, where we consider the Pomeron as a partonic probe. In this model:

$I\!P$-q interactions contribute to GW mass distribution.

$I\!P$-g interactions contribute to non GW, the high mass distribution.

THE PARTONIC POMERON

Current $I\!P$ models differ in details, but have in common a relatively large adjusted input $\Delta_{I\!P}$ and a diminishing $\alpha'_{I\!P}$.

Recall that, traditionally, $\Delta_{I\!P}$ determines the energy dependence of the total, elastic and diffractive cross sections while $\alpha'_{I\!P}$ determines the forward slopes. This picture is modified in updated $I\!P$ models in which s and t unitarity screenings induce a smaller $I\!P$ intercept at t=0, denoted $\Delta^{eff}_{I\!P}$, which gets smaller with energy. The exceedingly small fitted $\alpha'_{I\!P}$ implies a partonic description of the $I\!P$ which leads to a pQCD interpretation.

Gribov's partonic Regge theory provides the microscopic sub structure of the $I\!P$ where the slope of the $I\!P$ trajectory is related to the mean transverse momentum of the partonic dipoles constructing the Pomeron.

$$\alpha'_{I\!P} \propto 1/ < p_t >^2, \qquad \textbf{accordingly:} \qquad \alpha_S \propto \pi/ln\left(< p_t^2 > /\Lambda^2_{QCD}\right) << 1.$$

We obtain a $I\!P$ with hardness changing continuesly from hard (BFKL like) to soft (Regge like). This is a non trivial relation as the soft $I\!P$ is a moving pole in J-plane, while, the BFKL hard $I\!P$ is a branch cut, approximated, some times, as a simple pole with $\Delta_{I\!P} = 0.2 - 0.3$, $\alpha'_{I\!P} \simeq 0$.

GLM and KMR models are rooted in Gribov's partonic $I\!P$ theory with a hard pQCD $I\!P$ input. It is softened by unitarity screening (GLM), or the dependence of its partons' transverse momenta on their rapidity (KMR).

The two definitions are correlated.

GLM and KMR have a bound of validity, at 60(GLM) and 100(KMR) TeV, implied by their approximations. Consequently, as attractive as updated Pomeron models are, we can not utilize them above 100 TeV at the most.

To this end, the only relevant models are single channeled, most of which have a logarithmic parametrization input such as $[Aln(s) + Bln^2(s)]$.

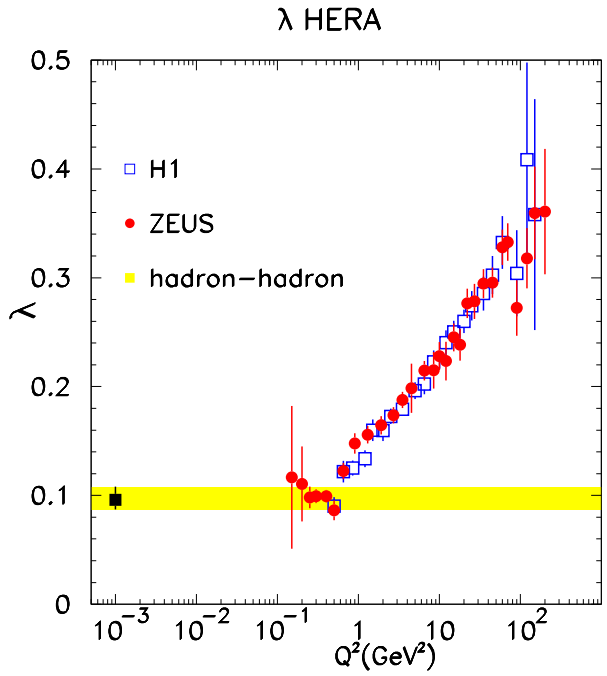

DIS: FROM SOFT TO HARD

The single $I\!P$ picture, suggested by GLM and KMR models, implies a smooth transition from the input hard $I\!P$ to a soft $I\!P$. In a different context, such a transition is supported by HERA dependence of $\lambda = \Delta_{I\!P}$ on Q^2 shown above.

Note, though, that a smooth transition from a soft to hard $I\!P$ can be reproduced also by a 2 $I\!P$s (soft and hard) model, such as Ostapchenko's.

UPDATED POMERON MODELS

Any discussion relating to phenomenological updated Pomeron models, has to distinguish between pre LHC and post LHC data.

To an extent, we observe a case in which a theoretical prejudice distorted the phenomenological interpratation of Fermilab raw data.

Consider $\sigma_{tot}(p\bar{p})$ at W=1.8 TeV:

Fermilab E710 measurement (PRD 1990) reported value was 72.1 $\pm$ 3.3 mb.

This value was supported (PLB 2002) by E811 who got 72.42 $\pm$ 1.55 mb.

CDF published (PRD 1994) a considerably higher value of 80.03 $\pm$ 2.24 mb.

The CDF number was rejected because its value was not consistent with the popular DL and COMPETE models.

The 1.8 TeV low value cross sections, were supported by all updated $I\!P$ models, which predicted that LHC soft pp cross sections would be considerably smaller than the actual TOTEM and ATLAS total and elastic pp cross sections.

Most models and parametrizations which reproduce TOTEM total and elastic cross sections, quoted below, are close to CDF cross sections at 1.8 TeV. TOTEM cross sections at 7 TeV are,

$$\sigma_{tot}(pp)=\mathbf{98.6\pm2.2mb}$$

$$\sigma_{el}(pp)=\mathbf{25.4\pm1.1mb}$$

They are supported by ATLAS cross sections,

$$\sigma_{tot}(pp)=\mathbf{95.4\pm1.4mb}$$

$$\sigma_{el}(pp)=\mathbf{24.0\pm0.6mb}$$

The TOTEM and ATLAS results force significant changes in the formulation of presently revised updated $I\!P$ models.

REVISED UPDATED POMERON MODELS

The desired improvement of the updated $I\!P$ models can be achieved by either improving the data fitting, or formulating the theoretical model, or both.

In the following I shall compare 6 updated Pomeron models, 3 by KMR and one each by GLM, Ostapchenko (OSTAP) and Kaidalov-Poghosian (KP). Note that, none of these models in their pre LHC version reproduced the TOTEM-ATLAS p-p cross sections. OSTAP and KP output are pre LHC. They had the largest cross sections which are not large enough to describe the TOTEM-ATLAS data.

- **GLM (Gotsman, Levin, Maor) operate with a single hard BFKL $I\!P$ input, in a 2 channel eikonal model. The hard input is softened by unitarity screenings. As we shall show, the model, as such, under estimates the TOTEM and ATLAS cross sections. GLM chose to modify their data fitting procedure by fixing the secondary Regge parameters from the low energy**

data base and then fit the $I\!P$ parameters from the over all data base. The output changes of the fitted parameters are not dramatic: $\Delta_{I\!P}$ changed from 0.21 to 0.23, and $\alpha'_{I\!P}$ changed from 0.0 to $0.028GeV^{-2}$. These relatively small changes enabled us to obtain an excellent reproduction of the elastic and diffractive soft cross sections in the ISR-LHC range.

- **KMR (Khoze, Martin, Ryskin) produced 3 single $I\!P$ models: One is a 2 channel eikonal model with $\Delta_{I\!P} = 0.11$, and $\alpha'_{I\!P} = 0.06GeV^{-2}$. The second is a 3 eikonal channel with $\Delta_{I\!P} = 0.14$, and $\alpha'_{I\!P} = 0.1GeV^{-2}$. The third model is an effective $I\!P$ model, based on non-enhanced eikonal which suppresses the growth of the soft cross sections. To this end KMR fix $\Delta_{I\!P} = 0.12$, and $\alpha'_{I\!P} = 0.05GeV^{-2}$.**

- **Ostapchenko has made (pre LHC) a comprehensive calculation in the framework of Reggeon Field Theory based on the resummation of both enhanced and semi enhanced $I\!P$ diagrams. To fit the elastic and diffractive cross sections he assumed 2 Pomerons (set C):** $\alpha^{soft} = 1.14 + 0.14t$ **and** $\alpha^{hard} = 1.31 + 0.085t$**.**

- **KP (Kaidalov and Poghosyan) model is based on Reggeon calculus. They describe the soft diffraction data taking all non enhanced absorptive corrections to the 3 Reggeon vertices and loop diagrams. It is a single $I\!P$ model with secondary Regge poles. Their $I\!P$ trajectory is determined by** $\Delta_{I\!P} = 0.12$ **and** $\alpha'_{I\!P} = 0.22 GeV^{-2}$**.**

- **A comparative table comparing the predictions of the models presented above follows in the next page.**

1.8 TeV	GLM	KMR14	KMR2C	OSTAP(C)	MBR*	KP
σ_{tot} (mb)	79.2	77.0	77.2	73.0	81.03	75.0
σ_{el} (mb)	18.5	17.4	17.4	16.8	19.97	16.5
σ_{SD} (mb)	11.27	3.4(LM)	2.82(LM)	9.2	10.22	10.1
σ_{DD} (mb)	5.51	0.2(LM)	0.14(LM)	5.2	7.67	5.8
B_{el} (GeV^{-2})	17.4	16.8	17.5	17.8		
7 TeV						
σ_{tot} (mb)	98.6	98.7	96.4	93.3	98.3	96.4
σ_{el} (mb)	24.6	24.9	24.0	23.6	27.2	24.8
σ_{SD} (mb)	14.88	2.6(LM)	3.05(LM)	10.3	10.91	12.9
σ_{DD} (mb)	7.45	0.2(LM)	0.14(LM)	6.5	8.82	6.1
B_{el} (GeV^{-2})	20.2	19.7	19.8	19.0		19.0
14 TeV						
σ_{tot} (mb)	109.0	112.7	108.	105.	109.5	108.
σ_{el} (mb)	27.9	30.1	27.9	28.2	32.1	29.5
σ_{SD} (mb)	17.41	3.5(LM)	3.15(LM)	11.0	11.26	14.3
σ_{DD} (mb)	8.38	0.2(LM)	0.14(LM)	7.1	9.47	6.4
B_{el} (GeV^{-2})	21.6	21.6	21.1	21.4		20.5

UNITARITY SATURATION

Unitarity saturation is coupled to 3 experimental signatures:

$\frac{\sigma_{inel}}{\sigma_{tot}} = \frac{\sigma_{el}}{\sigma_{tot}} = 0.5,\ \frac{\sigma_{tot}}{B_{el}} = 9\pi,\ \sigma_{diff}$**=0 in a multi-channel model.**

Following is p-p TeV-scale data relevant to the assessment of saturation:

CDF(1.8 TeV): $\sigma_{tot} = 80.03 \pm 2.24mb,\ \sigma_{el} = 19.70 \pm 0.85mb,\ B_{el} = 16.98 \pm 0.25GeV^{-2}.$

TOTEM(7 TeV): $\sigma_{tot} = 98.3 \pm 0.2(stat) \pm 2.8(sys)mb,\ \sigma_{el} = 24.8 \pm 0.2(stat) \pm 2.8(sys)mb,$

$B_{el} = 20.1 \pm 0.2(stat) \pm 0.3(sys)GeV^{-2}.$

ATLAS(7 TeV): $\sigma_{tot} = 95.4 \pm 1.4mb, \quad \sigma_{el} = 24.0 \pm 0.6mb.$

AUGER(57 TeV): $\sigma_{tot} = 133 \pm 13(stat) \pm^{17}_{20} sys \pm 16(Glauber)mb,$

$\sigma_{inel} = 92 \pm 7(stat) \pm^{9}_{11} (sys) \pm 16(Glauber)mb.$

We get: $\frac{\sigma_{inel}}{\sigma_{tot}}$ **=0.754(CDF), 0.748(TOTEM), 0.748(ATLAS), 0.692(AUGER).**

The numbers above suggest a very slow approach toward saturation, well above the TeV-scale. Consequently, the study of pp saturation depends on information above the TeV-scale.

There are 2 sources from which we may obtain the desired information:

- **Cosmic Rays data. Recall that p-p cross sections obtained from p-Air data have relatively large margin of errore. AUGER p-p cross sections are a good example.**
- **Since updated $I\!P$ models are confined to the TeV-scale, p-p cross sections at higher energies can be calculated only in single channeled models, the deficiencies of which have been stated before.**

Out of a few single channeled nodels, I shall quote Block and Halzen (BH), which reproduce well the inelastic and total cross sections at the TeV-scale. The BH model can be applied at exceedingly high energies.

The prediction of BH at the Planck-scale ($\mathbf{1.22}\cdot 10^{16} TeV$) is:

$$\sigma_{inel}/\sigma_{tot} = 1131mb/2067mb = \mathbf{0.547.}$$

It indicates that saturation will be attained, if at all, at non realistic energies.

The predicted multi channel vanishing of the diffractive cross sections at saturation implies that σ_{sd}, which up to the TEVATRON grows slowly with energy, will eventually start to reduce.

This may serve as an early signature that saturation is being approached. Specifically, the preliminary TOTEM measurement of

$$\sigma_{sd} = 6.5 \pm 1.3mb$$

$$3.4 < M_{sd} < 1100GeV$$

$$2.4 \cdot 10^{-7} < \xi < 0.025$$

suggests a radical change in the energy dependence of $\sigma_{sd}/\sigma_{inel}$ which is considerably smaller than its value at CDF.

$$\sigma_{sd}/\sigma_{inel} = \textbf{0.151(CDF), 0.088(TOTEM).}$$

This feature, if correct, is, presently, particular to diffraction. It suggests a much faster approach toward unitarity saturation than suggested by $\frac{\sigma_{inel}}{\sigma_{tot}}$.

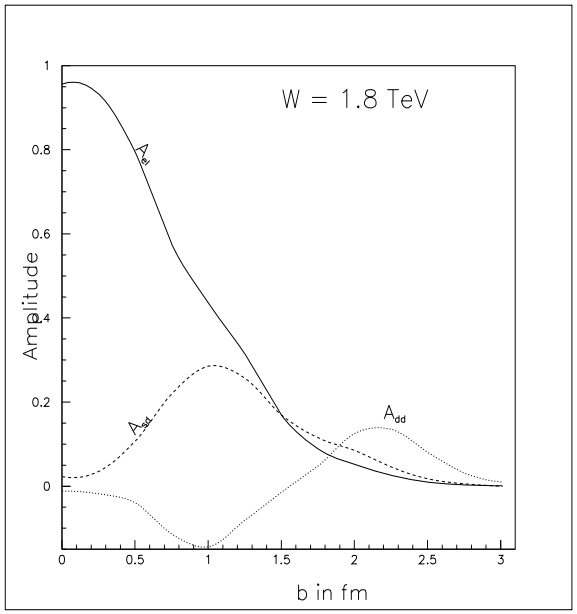

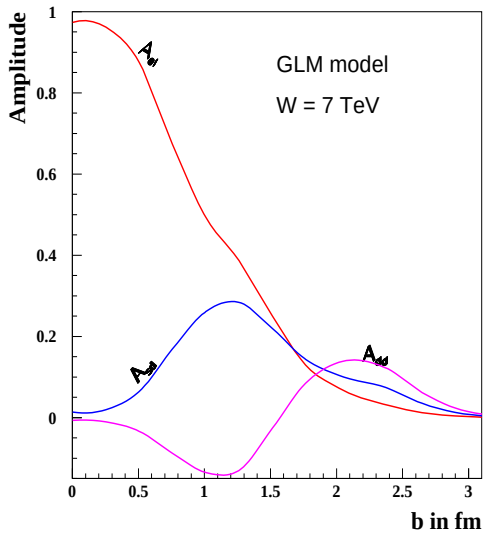

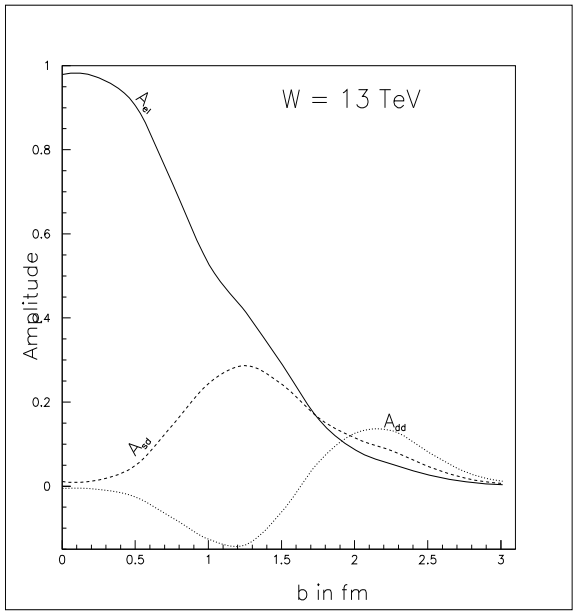

TOTEM diffractive data is very preliminary. Regardless, the compatibility between the information derived from different channels of soft scattering deserves a very careful study!

The figures above show the GLM elastic, SD and DD b-amplitudes at 1.8, 7 and 14 TeV. The difference between our output and competing models is not dramatic. The GLM SD cross sections (in mb) are:

$\sigma_{sd}(W) = \sigma_{sd}^{GW} + \sigma_{sd}^{nonGW} =$ $9.2 + 1,95(1.8)$, **10.7+4.18(7)**, $11.5 + 5.81(14)$.

Recall that, EL, SD and DD cross section values are obtained from a b^2 integration of the corresponding amplitude square. The growth of σ_{sd}, as a function of W, is mainly a consequence of $a_{sd}(s,b)$ moving slowly toward higher b values. The net result is a continuation of SD moderate increase with energy.

Consequently, I do not expect a suppression of σ_{sd} at an energy of 7 TeV, as inplied by TOTEM sd data and recent KMR papers.

An early reduction of the diffractive channels at relatively low energies, will require, thus, a fundamental change in our interpretation of soft scattering at the TeV-scale.

A summary of GLM results followes.

$\sqrt{s}$ TeV	1.8	7	8
σ_{tot} mb	79.2	98.6	101.
σ_{el} mb	18.5	24.6	25.2
$\sigma_{sd}(M \leq M_0)$ mb		$10.7+(2.8)^{nGW}$	$10.9+(2.89)^{nGW}$
$\sigma_{sd}(M \leq 0.05s)$ mb	$9.2+(1.95)^{nGW}$	$10.7+(4.18)^{nGW}$	$10.9+(4.3)^{nGW}$
σ_{dd} mb	$5.12+(0.38)^{nGW}$	$6.2+(1.166)^{nGW}$	$6.32+(1.29)^{nGW}$
B_{el} GeV^{-2}	17.4	20.2	20.4
B_{dl}^{GW} GeV^{-2}	6.36	8.01	8.15
σ_{inel} mb	60.7	74.	75.8
$\frac{d\sigma}{dt}\|_{t=0}$ mb/GeV^2	326.34	506.4	530.7
$\sqrt{s}$ TeV	13	14	57
σ_{tot} mb	108.0	109.0	130.0
σ_{el} mb	27.5	27.9	34.8
$\sigma_{sd}(M \leq 0.05s)$ mb	$11.4+(5.56)^{nGW}$	$11.5+(5.81)^{nGW}$	$13.0+(8.68)^{nGW}$
σ_{dd} mb	$6.73+(1.47)^{nGW}$	$6.78+(1.59)^{nGW}$	$7.95+(5.19)^{nGW}$
B_{el} GeV^{-2}	21.5	21.6	24.6
σ_{inel} mb	80.5	81.1	95.2
$\frac{d\sigma}{dt}\|_{t=0}$ mb/GeV^2	597.6	608.11	879.2